Electrically tunable directional light scattering from soft thin membranes

LEIHAO CHEN,[1,2] JAMES J. C. BUSFIELD,[1] FEDERICO CARPI[2,*]

[1]*School of Engineering and Materials Science, Queen Mary University of London, Mile End Road, London, E1 4NS, UK*
[2]*Department of Industrial Engineering, University of Florence, Via di S. Marta 3, Florence, 50139, Italy*
**federico.carpi@unifi.it*

Optics Express Vol. 28, No. 14 / 6 July 2020, 20669

https://doi.org/10.1364/OE.392015

ACCEPTED VERSION

Abstract: The possibility to electrically tune the scattering of light from surfaces by dynamically varying their properties is desirable for controllable transparency devices and diffusion filters. As a difference from state-of-the-art approaches where scattering is changed isotropically, this paper presents the first smart-material-based technology enabling electrical modulations in a single or multiple directions, which can be selected dynamically. The effect is achieved from thin soft membranes with transparent PEDOT:PSS coatings, which are electrically deformed along a single or multiple axes, using dielectric elastomer actuation. Anisotropic scattering is induced by electrically tuning the formation of directional surface wrinkles. As a proof of concept, a bi-directional device is obtained by overlapping two 90°-shifted mono-directional layers that can be controlled independently. According to the activation of the layers, light can be scattered along either direction, as well as both of them. Prototypes made of an acrylic elastomer were demonstrated with mono- and bi-directional operations. Devices with a window-to-total area ratio of 1:4 also showed a maximum electrical reduction of optical transmittance from 75% to 4%. This functionality and possible extensions to more than two controllable directions suggest applicability as electrically controllable anisotropic light diffusers for dynamic light shaping, as well as tunable transparency surfaces.

1. Introduction

Smart devices capable of tuning the scattering of light by means of a control voltage are gathering significant interest for various applications, including controllable transparency devices (such as dimmable windows and privacy glasses) and controllable light diffusing filters [1–3]. The most used technologies for such optical devices consist of electrochromic materials [4–6] and polymer-dispersed liquid crystals (PDLC) [7–10]. Recently, so-called dielectric elastomer actuators (DEAs) have been reported as a promising alternative technology to obtain voltage-induced large and continuous changes of the transparency of a soft surface [11–19]. Unlike electrochromic materials, where the operation is based on electrochemical reactions, the DEA technology relies on an electrostatic effect, which is therefore intrinsically faster [11–19]. In comparison with PDLC materials, which only offer on-off switching capabilities, DEA-based devices allow for the transparency to be controlled over continuous ranges [11–19].

As a type of electromechanically active polymer (EAP) actuators [20], DEAs essentially are deformable capacitors made of a dielectric elastomer (DE) membrane, typically consisting of acrylic or silicone elastomers, coated on both sides with deformable electrodes. The latter can be made of transparent materials (including graphene, carbon nanotubes, ionic conductors, silver nanowires or conducting polymers) or not (for example, carbon loaded elastomers or greases) [21]. As an electric field is applied through the membrane, an electrostatic stress causes the elastomer to undergo a reversible surface expansion and thickness compression [22,23]. That stress is determined by the applied electric field E and the dielectric permittivities of the elastomer ε_r and vacuum ε_0, as follows: $p = \varepsilon_0 \varepsilon_r E^2$ [23]. In general, devices based on the DEA technology can exhibit large actuation strains, high response speeds, light weight, high resilience, high energy efficiency and no acoustic noise [24–28].

State-of-the-art approaches that use DEAs to electrically control the optical transmittance of an elastomeric membrane could be divided in two main groups: tuneable diffraction and tuneable scattering. In the former, a DEA is employed to vary the period of a deformable diffractive grating, achieving electrically-controllable structural colorations [29–31]. Being such an aim not relevant to the work presented here, this group will not be further considered in the following.

Differently, the second group consists of devices where DE actuation modulates the scattering of light from a soft membrane, to achieve electrically-controllable changes of transparency. They exploit the following four working principles. In a first strategy, a DE membrane is made translucent with wrinkled stretchable transparent electrodes, whose transparency can be increased by voltage-induced surface expansions that flatten the wrinkles [11–13]. The second strategy combines the previous concept with a compression of the membrane by an outer annular DEA, so as to obtain a dual-operation device, whose transparency can be both increased and decreased, depending on whether the electrical activation is used to generate a membrane expansion or contraction [14]. The third strategy uses transparent electrodes that cover a DE membrane fixed to a rigid glass substrate, whose transparency can be reduced by very high electric fields, which create microscopic craters on the surface, due to electromechanical instabilities [15–18]. The fourth strategy uses electric field-induced alignments of liquid crystals encapsulated within a DE membrane sandwiched between transparent electrodes, so as to switch the membrane's appearance from opaque to transparent [19].

All these strategies lead to a scattering of light that is isotropic over the entire membrane. Whilst this feature complies, for instance, with the typical requirements of smart windows for electrically dimmable transparency, it introduces limitations when being considered for different applications, such as controllable light diffusers. Indeed, it could be of interest to electrically tune the diffusion along selectable directions, for various needs, such as to avoid direct spot lights or to obtain directional soft illumination [3].

In order to enable that functionality, here we present a concept that uses dielectric elastomer actuation to electrically tune the anisotropy of scattering, achieving directional scattering. As a demonstrator, a bi-directional device able to orient the diffusion along two orthogonal selectable directions is described. Moreover, we show that the device allows for electrically controlling the optical transparency within a broad range.

2. Methods

2.1 Structure and principle of operation

The proposed bi-directional device is obtained by overlapping two 90°-shifted mono-directional light scattering layers, which can be controlled independently.

Fig. 1(a) presents the structure of each mono-directional layer, consisting of a thin soft (elastomeric) membrane, which is uniaxially pre-stretched, clamped to a rigid support frame and coated with different materials. In particular, a square central area, acting as a 'window' with tunable size, is coated on both sides with a deformable transparent medium having strain-dependent scattering properties. This area is interposed between two lateral rectangular regions, where both sides of the membrane are coated with a non-transparent stretchable conducting material (dark rectangles in Fig. 1(a)). These two lateral regions correspond to two deformable capacitors, acting as DEA segments. They can compress the central part of the membrane (window) in response to an applied voltage, as described below.

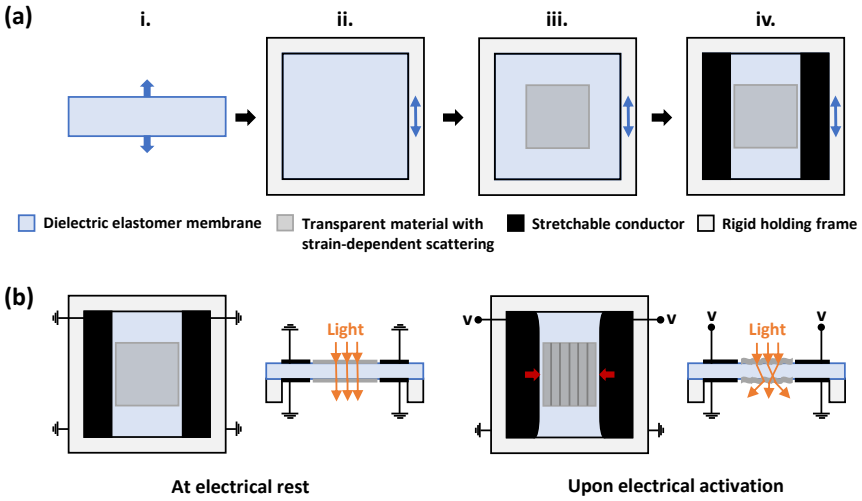

Fig. 1. Proposed DEA-based device to achieve an electrically tunable mono-directional light scattering from a soft thin membrane. (a) Fabrication steps, consisting of: i) uniaxial pre-stretching (blue arrows) of the membrane; ii) application of a rigid holding frame; iii) deposition, on both sides, of a transparent material with strain-dependent scattering properties; iv) creation, on both sides, of two lateral coatings with a non-transparent stretchable conductor. (b) Top and cross-sectional views illustrating the working principle: at electrical rest, the central window made up of the coated membrane is optically transparent, whilst an electrical activation of the two lateral regions compresses it along one direction (red arrows); this creates uni-directional wrinkles (schematically indicated as parallel lines on the surface), which scatter light mostly along the direction of contraction. Moreover, the membrane shows a lower transparency. Note: the (non-uniform) change of thickness of the membrane due to its actuation is not shown for simplicity.

The principle of operation of this mono-directional light scattering layer is presented in Fig. 1(b). At electrical rest (no applied voltage), the central coating is such that the coated membrane has a certain transparency. By electrically driving both the lateral DEA segments, the central window is deformed anisotropically. In particular, a combination of two effects maximizes the expansion of the DEA segments orthogonally to the membrane's pre-stretch direction: one effect is due to the constraints imposed by the frame at three edges of the rectangular segments (Fig. 1); the other effect is due to the membrane's stiffening along the pre-stretch direction, which makes the electrically induced deformation to occur primarily along the orthogonal direction [22,32]. Therefore, in response to an applied voltage, the expansion of the DEA segments causes a contraction of the central window along the direction without pre-stretch (Fig. 1(b)). If the stiffness of the central coating is higher than that of the elastomer membrane (as a consequence of a difference in elastic modulus and/or thickness), the resulting effect is the generation of uni-directional wrinkles, which mostly scatter light along the direction of contraction. This mono-directional scattering corresponds also to a reduction of the coated membrane's transparency.

It is worth noting that coating the membrane with a scattering material is necessary, as the naked elastomeric surface might not show sufficient wrinkling due to the contraction and therefore might not be able to significantly scatter light (as shown by the comparative tests presented later).

In order to obtain a bi-directional device, two mono-directional layers are overlapped with a 90° shift, as shown in Fig. 2. An air gap is maintained between the layers, so as to make them able to deform independently from each other, in order to avoid a mutual constraining effect.

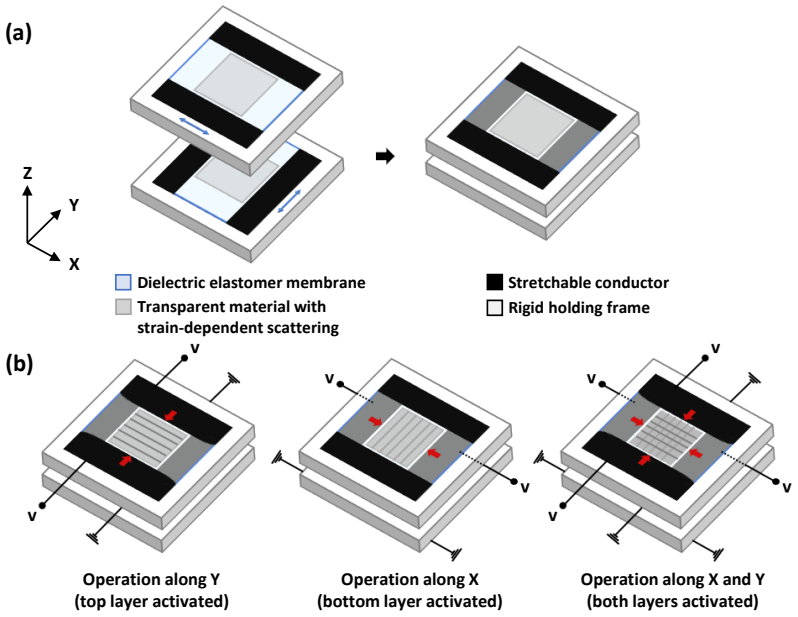

Fig. 2. Proposed DEA-based device to achieve an electrically tunable bi-directional light scattering from a soft thin membrane: (a) assembly of the device, by overlapping two mono-directional layers shifted by 90°; (b) mono- and bi-directional operation modes of the device, obtained by electrically wrinkling one or both the layers, respectively. The uni-directional wrinkling of a layer is schematically indicated as parallel lines on its surface. The red arrows indicate the direction of the maximum electrically-induced deformation of the rectangular DEAs.

The two mono-directional layers can electrically be controlled independently, so as to enable both mono- and bi-directional operations of the device. Therefore, depending on whether the electrical activation of the two layers is mutually exclusive or simultaneous, light can be scattered along either one of the two selectable orthogonal directions, or along both of them simultaneously.

2.2 Materials

Prototype samples of the proposed device were fabricated as follows. The dielectric elastomer membrane consisted of a commercially available transparent acrylic elastomer film (VHB 4905, 3M, USA), having a thickness of 500 µm at electrical rest. This test membrane, which is widely used in the DEA field, was selected as a convenient test material, due to its high electromechanical transduction performance in quasi-static conditions [22–26] and its adhesive properties, which simplified the manufacturing process.

To obtain the central tunable window, the membrane was coated with a thin film of a transparent material having strain-dependent scattering properties, consisting of poly(3,4-ethylenedioxythiophene):poly(styrenesulfonate) (PEDOT:PSS). This material can reach high optical transmittances and is widely used for transparent deformable conductive layers in flexible electronics [33–35]. Furthermore, the refractive indexes that it can reach make it a good choice for the intended application in this work: when it is deposited as thin films on surfaces with highly variable wrinkling, the widely tunable scattering that can be achieved offers a broad tuning range of optical transmittance, as also demonstrated by the test results presented in the following.

The coating was achieved by spraying (with an airbrush) a PEDOT:PSS compound, consisting of an aqueous PEDOT:PSS solution (Clevios PH 1000, Heraeus, Germany) in which the solid content was 1-1.3 wt%, with addition of 5 wt% dimethyl sulfoxide (DMSO,

Sigma-Aldrich, UK) and 40 wt% fluorosurfactant (Capstone FS-30, Apollo Scientific, UK). The compound was diluted in isopropanol (2-Propanol, Sigma-Aldrich, UK) with a ratio of 1:3 by weight to prepare the spray solution.

It is worth noting that the PEDOT:PSS coating was also electrically conductive. Nevertheless, its conductivity was not used, as the principle of operation only required a deformable transparent medium with strain-dependent scattering properties. Therefore, even non-conductive materials could have been chosen. However, in this work PEDOT:PSS was adopted to enable comparisons with a previous work of ours [14], where it had been used both as a scattering medium and as a deformable electrode.

The non-transparent stretchable electrodes were obtained by coating the membrane with conductive carbon grease (846, M.G. Chemicals, Canada).

2.3 Fabrication of the device

A mono-directional light scattering device (single layer) was fabricated as shown in Fig. 1(a). A rectangular sample (60 mm × 15 mm) of the elastomer membrane was uniaxially pre-stretched by 4 times and fixed to a square support frame (60 mm × 60 mm, internally), taking advantage of the membrane's adhesive properties. The applied pre-stretch reduced the membrane thickness from 500 to 125 µm (calculated value).

A volume of 32 µl of the PEDOT:PSS solution was sprayed on each side of the pre-stretched membrane, previously covered with a mask, obtaining in a central square region (30 mm × 30 mm) a thin coating.

The thickness of the coating was estimated as follows. By considering the typical density of the solution's components and their proportion by weight, their proportion by volume was calculated and used to estimate the solution's volume fraction (0.18%) that was deposited as a PEDOT:PSS solid film, after evaporation of the volatile components. Assuming that the deposited film covered exactly the central window (30 mm × 30 mm), the resulting thickness would be 64 nm. However, that number is an overestimate, as a fraction of the material also partially covered the mask and so was lost. Therefore, it is reasonable to consider that the actual thickness of the window coating was lower than 100 nm.

It is worth noting that the PEDOT:PSS coating was applied to both sides, although in principle this was not necessary. Indeed, this was found to be a suitable approach to maximize the tuneable range.

Considering the size of the central window (30 mm × 30 mm) and that of the framed membrane (60 mm × 60 mm), the window-to-total area ratio of the device was 1:4.

To obtain the DEA electrodes, the conductive carbon grease was applied on two lateral rectangular regions (13 mm × 60 mm) of both sides of the membrane. The edge of each electrode was separated by the edge of the central transparent coating by a gap of 2 mm (Fig. 1a), so as to avoid electrical continuity, due to the PEDOT:PSS conductivity. Whilst that gap was sufficient to operate in air the prototype devices tested in this work, it could be reduced with insulating coatings. This would reduce the length of the inactive region between the electrodes and so maximise the electrically achievable compressive strain of the central window, for any given size (and, so, active deformation) of the electrodes.

The sample was then oven-dried for 30 min at 80 °C, in order to extract the PEDOT:PSS solvent. A copper tape was used to create electrical contacts on each electrode for connection to the voltage source.

The bi-directional device was obtained by aligning two mono-dimensional layers with a 90°-shift, as shown in Fig. 2. The spacing between the two layers was 3 mm.

2.4 Electrical driving

A compact DC-DC high voltage converter (Q50, EMCO High Voltage Corporation, USA) was used to produce voltages up to 4 kV, which were monitored with a high-voltage probe.

Each voltage value was divided by the elastomer membrane's thickness at electrical rest (125 µm) to calculate the nominal electric field generated within the DEAs.

2.5 Electro-mechanical characterisation

The central window's axial strains, representing the variation of the distance between the inner edges of the two rectangular electrodes, were estimated by taking pictures at different voltages and processing the images via the Fiji-ImageJ open-source software.

2.6 Electro-optical characterisation

The electrically-induced changes in the optical transmittance of the elastomer membrane were quantified in the 400-800 nm visible range, using a Perkin Elmer Lambda 950 UV-vis spectrometer with a 10 cm-wide integrating sphere. Both near-field and far-field measurements, corresponding to a sample-to-detector distance of 5 and 40 cm, respectively, were performed, as shown in Fig. 3.

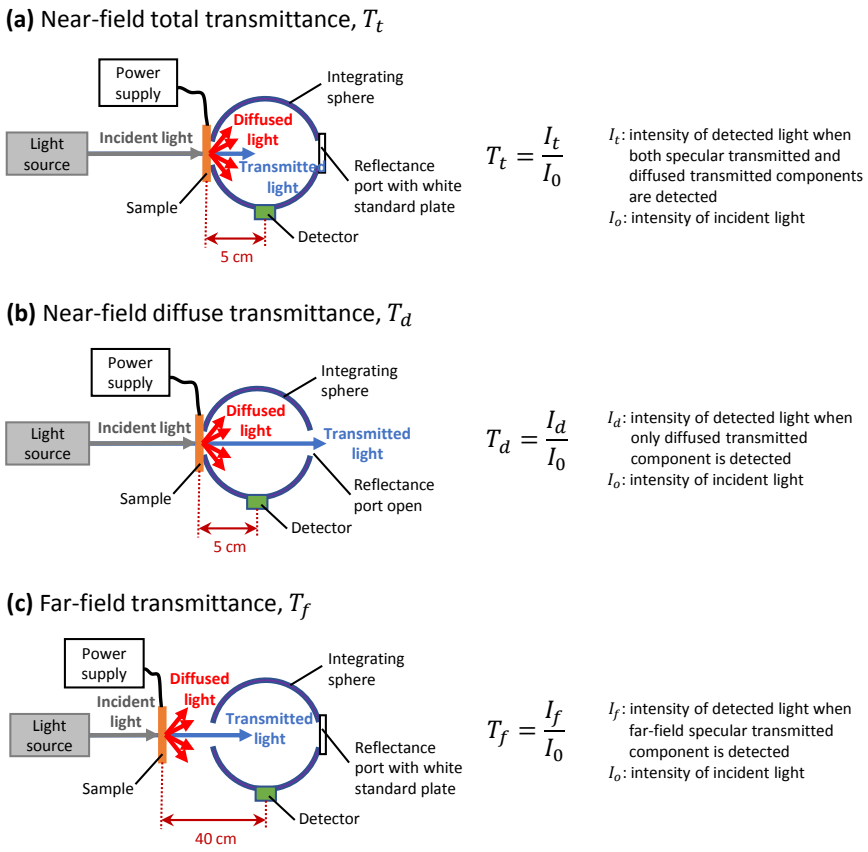

Fig. 3. Schematic representation of the UV-Vis spectrometer set-up used to characterize the transmittance: (a) Near-field total transmittance measurement, with both specular transmitted and diffused transmitted light detected; for this test, the transmission port was covered with the sample, whilst the reflectance port was covered with a white standard plate. (b) Near-field diffuse transmittance measurement, with only diffused transmitted light detected; for this test, the transmission port was covered with the sample, whilst the reflectance port was left open. (c) Far-field transmittance measurement, with only specular transmitted light detected; for this test, the transmission port was left open, whilst the reflectance post was covered with a white standard plate.

The near-field measurements included both the diffuse transmittance T_d (percentage of incident light transmitted as diffused light) and the total transmittance T_t (percentage of incident light transmitted as a whole, including both diffused transmitted and specular transmitted components, i.e. both scattered and not), which were detected as described in Fig. 3. The ratio between the near-field diffuse and total transmittances was calculated to obtain the transmission Haze $H = T_d/T_t$. This ratio, expressing the portion of total transmitted light that propagates as diffused light, was used as a quantification of the cloudy appearance of the sample [36].

In the far-field measurements, the increased sample-to-detector distance was such that the diffused transmitted component was mostly lost by the measurement apparatus, which therefore basically detected only the specular transmitted component (Fig. 3). Thus, the far-field transmittance T_f essentially represented the percentage of incident light transmitted as specular component, as also confirmed by the experimental data reported in the following.

2.7 Microscopic investigations

The formation of surface wrinkles within the PEDOT:PSS coating at different axial strains was investigated using an atomic force microscope – AFM (NanoWizard 4 BioAFM, JPK Instruments AG, Germany) and a scanning electron microscope – SEM (Inspect F50, FEI, USA). The AFM images were taken with a cantilever probe (NSG01, NT-MDT, Russia) having a resonant frequency of around 150 kHz and a spring constant of 3.5 N/m. Owing to the PEDOT:PSS conductivity, for the SEM investigations the samples did not require any further coating with additional conductors.

The tests were made on an electrically passive sample used as a dummy device, to be deformed mechanically rather than electrically. Indeed, deforming the central widow electrically during AFM and SEM testing would be too challenging, owing to an incompatibility between the procedures/equipment and the high voltage driving of the device. The sample was fabricated as follows. A uniaxially pre-stretched and PEDOT:PSS-coated membrane was fixed to a plastic frame, according to the layout described above, although it was not provided with the DEA electrodes. The window was then manually contracted along the pre-stretch direction, by pulling the two edges of the coated layer towards each other using two small plastic bars attached to the membrane and keeping them in place with other plastic bars to maintain the contraction. This way, the PEDOT:PSS coating was subject to a set of axial strains analogous to those experienced by the device upon electrical activation: -2.5%, -5%, -7.5% and -10%. In addition, the strain was reversed back to 0%, by completely releasing the contraction, so as to investigate the surface wrinkling reversibility.

3. Results and discussion

3.1 Electro-mechano-optical performance of the mono-directional device

The electro-mechano-optical transduction performance of the mono-directional device is presented in Fig. 4, where it is also compared with that of a device without PEDOT:PSS coating, tested as a control sample.

From a qualitative standpoint, the electrical tuneability of the device transparency can be appreciated from the photos in Fig. 4(a), which show, as an example, the progressive blurring of a text behind the window, as a result of the electrically-induced progressive scattering of light. Fig. 4(b) plots the dependence on the applied electric field of the geometrical variable that caused the effect, i.e. the axial strain of the window along its direction of maximum contraction.

The quantification of the optical effect is presented in Figs. 4(c) and 4(d), which show the variation of the transmittances with the applied field. In particular, at electrical rest the device had rather high near-field total and far-field transmittances (around 86%), due to the transparency of the PEDOT:PSS coating. By increasing the applied voltage, a growing

scattering of the transmitted light caused a progressive rise of the near-field diffuse transmittance (red line in Fig. 4(c)), consistently paralleled by a progressive drop of the far-field transmittance (blue line in Fig. 4(c)), down to about 21%.

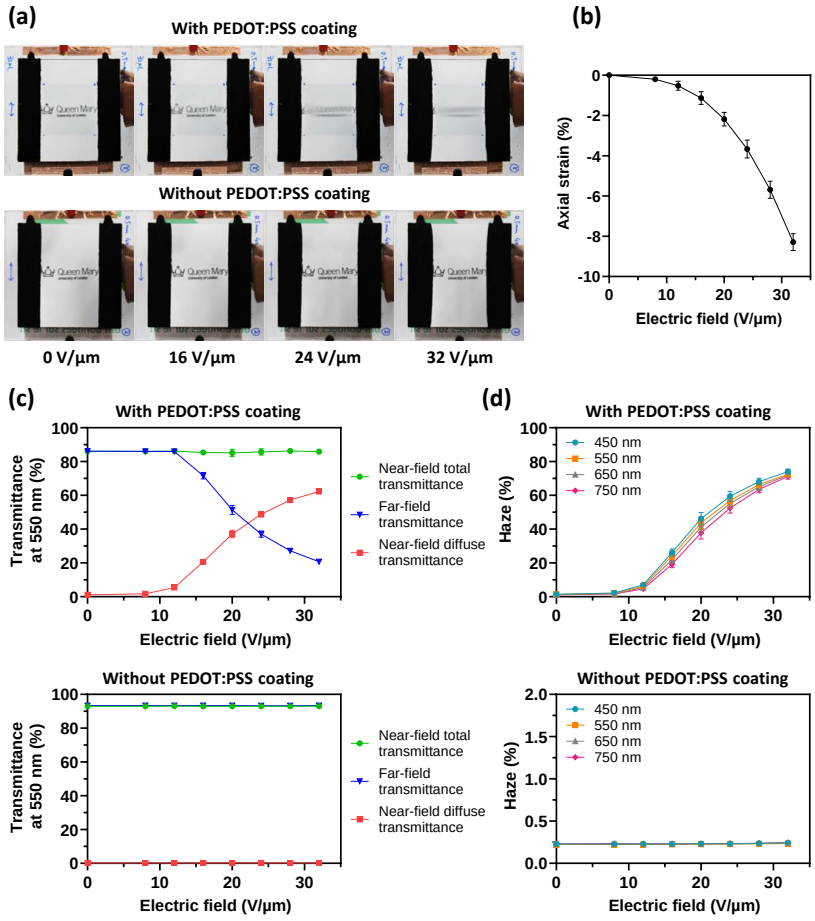

Fig. 4. Electro-mechano-optical transduction performance of the mono-directional light scattering device and comparisons between samples with and without PEDOT:PSS coating: (a) Photos showing the achieved reduction of transparency in response to increasing nominal electric fields; the visualized text was located 3 cm behind the window; (b) Effect of the applied electric field on the central window's axial strain (variation of the distance between the inner edges of the lateral electrodes) along the direction of maximum contraction; (c) Electrically-induced variations of the transmittances (near-field total, near-field diffuse and far-field) at 550 nm; (d) Dependence on the applied nominal electric field of the Haze number at different wavelengths. Each data point represents the average value from three sample devices. Error bars corresponding to the standard deviation are included, although most of them are too small to be seen.

The sum of the near-field diffuse and far-field transmittances corresponded, with a high accuracy (±5% error), to the near-field total transmittance (green line in Fig. 4(c)). This implies that, in the far field, the sample-to-detector distance (40 cm) was sufficiently long that in practice all the detected light was only the specular transmitted component, without any diffuse component (Fig. 3). Therefore, the resulting far-field transmittance is indicative of the transparency that an observer would perceive while looking through the device window, perpendicularly to it, from that distance.

The cloudy appearance of the device resulting from the electrically induced higher scattering is quantified by the Haze-field plots presented in Fig. 4(d).

As a comparison, the control sample without any PEDOT:PSS coating showed, for each applied field, constant near-field total and far-field transmittances of about 92% at 550 nm, and, consistently, a practically null diffuse transmittance (Fig. 4(c)). Likewise, the Haze value was practically null (Fig. 4(d)). These data indicate that the coating is necessary in order to provide the membrane's surface with scattering properties.

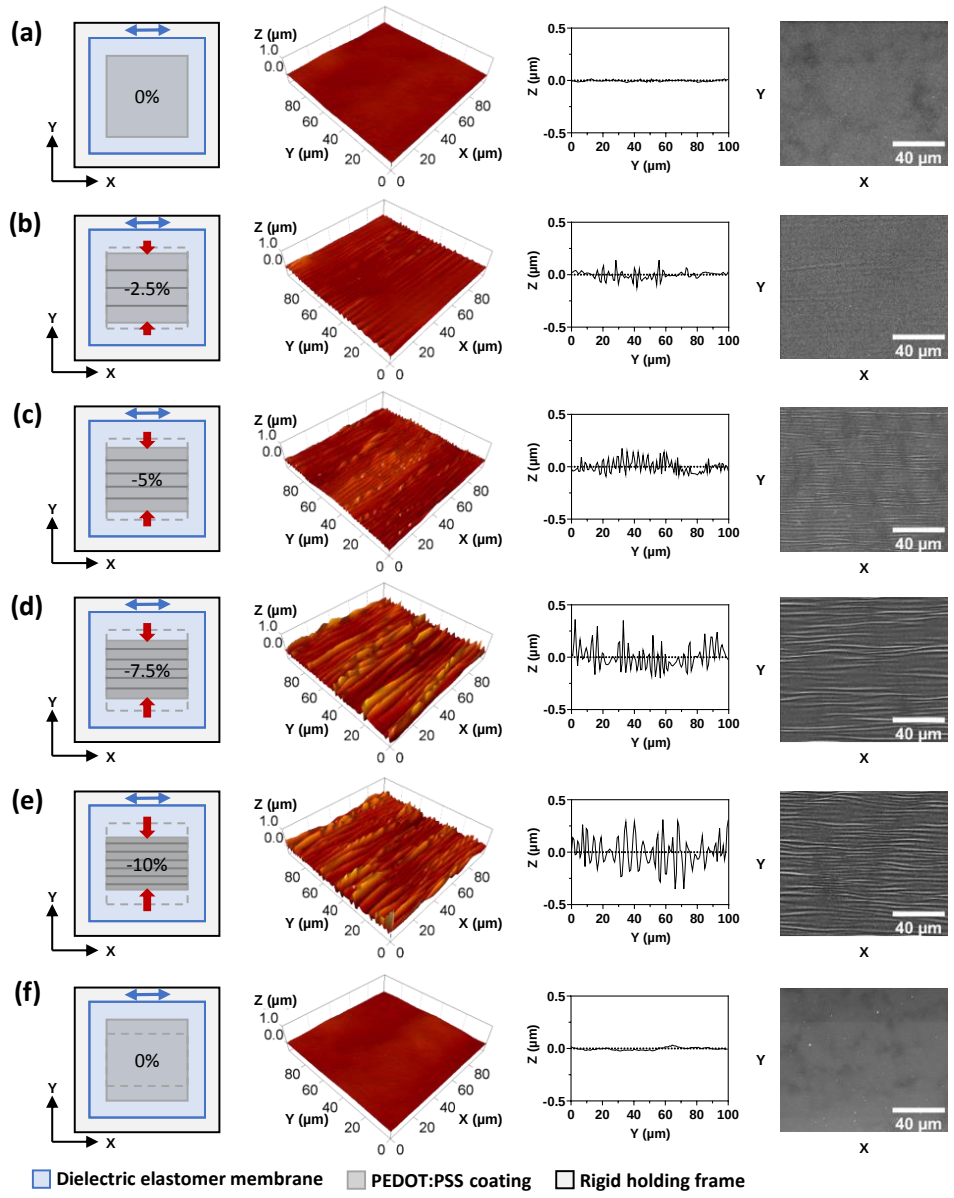

Fig. 5. Microscopic investigations on the reversible wrinkling of the PEDOT:PSS coating of the elastomer membrane uniaxially pre-stretched along the direction X (blue arrows), as a result of different contraction strains imposed along the direction Y (red arrows). The uni-directional wrinkling of the coating is schematically indicated as parallel lines on its surface (first column). AFM plots (second and third columns) and SEM images (fourth column) of the surface are shown at an axial strain of (a) 0%, (b) -2.5%, (c) -5%, (d) -7.5%, (e) -10% and then back to (f) 0%.

It is worth stressing that the achieved performance depended, for any given applied electric field, on the extent of the deformation of the central window, and, so, on that of the lateral actuation segments. Thereby, the maximum variation of transmittance was determined by the size of those segments. That size is a design parameter, whose selection should of course take into account the admissible encumbrance of the whole device. The prototype samples tested in this work had a window-to-total area ratio of 1:4.

3.2 Microscopic investigations on surface wrinkling

Results of the AFM and SEM investigations on the reversible formation of surface wrinkles on the PEDOT:PSS coating at various axial strains are presented in Fig. 5.

The images show that the PEDOT:PSS coating was initially smooth (Fig. 5(a)) and then, for increasing contraction strains, it exhibited progressive uni-directional wrinkling (Figs. 5(b)-(e)). The wrinkles' height gradually increased from about 0.1 µm at a -2.5% strain to about 0.4 µm at a -10% strain. These morphological changes were fully reversible, as they disappeared when the strain was reverted back to 0% (Fig. 5(f)).

As the strains experimented in these tests were analogous to those achieved with an electrical actuation of the device, these results confirm that the electrical tuneability of the coated membrane's transparency is due to changes of topographic patterns, which can be controlled continuously and reversibly.

It is worth pointing out that no significant wrinkles could be created without a PEDOT:PSS coating, as shown by the control test presented in Fig. 6. So, the fact that the coating was necessary to achieve scattering (as shown by the optical tests presented in Fig. 4) can be explained with the evidence that PEDOT:PSS is needed to create wrinkles, which otherwise cannot be achieved by simply compressing an uncoated membrane. The wrinkles result from buckling of the stiffer coating material.

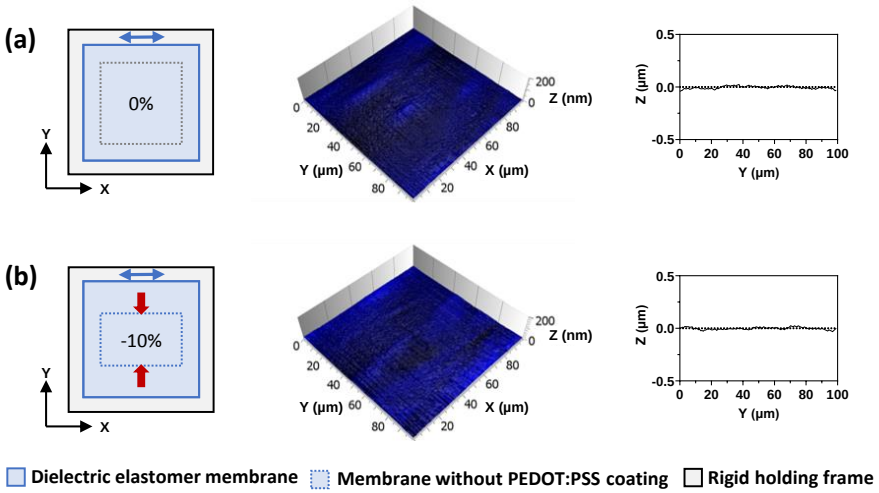

Fig. 6. AFM investigation on a membrane without PEDOT:PSS coating, as a control test. The membrane was uniaxially pre-stretched along the direction X (blue arrows) and the contraction strain was imposed along the direction Y (red arrows). AFM plots (second and third columns) of the surface are shown at an axial strain of (a) 0% and (b) -10%.

3.3 Electro-optical performance of the bi-directional device

The performance of the bi-directional device is presented in Figs. 7, 8 and 9, which refer to electrical activations of, respectively, only the rear layer, only the front layer and both layers simultaneously.

In particular, a grid was imaged through the device to show how a uni-directional compression of the window was able to selectively emphasize uni-directional features, like the vertical and horizontal lines, which could be independently isolated. A light spot, which was varied from a circle to a line or a cross, was used to demonstrate how a directional driving of the device can be used for an electrically controllable directional shaping of light (light beam spreading). Finally, a flower was used as an object without dominant features in the two working directions of the device to show the difference in blurring achievable with a uni- or bi-directional driving.

The degree of controllability of the device can also be evaluated from the supplementary video (Visualization 1), which shows directional progressive blurring of the grid pattern imaged through the device, as also presented in Figs. 7 to 9.

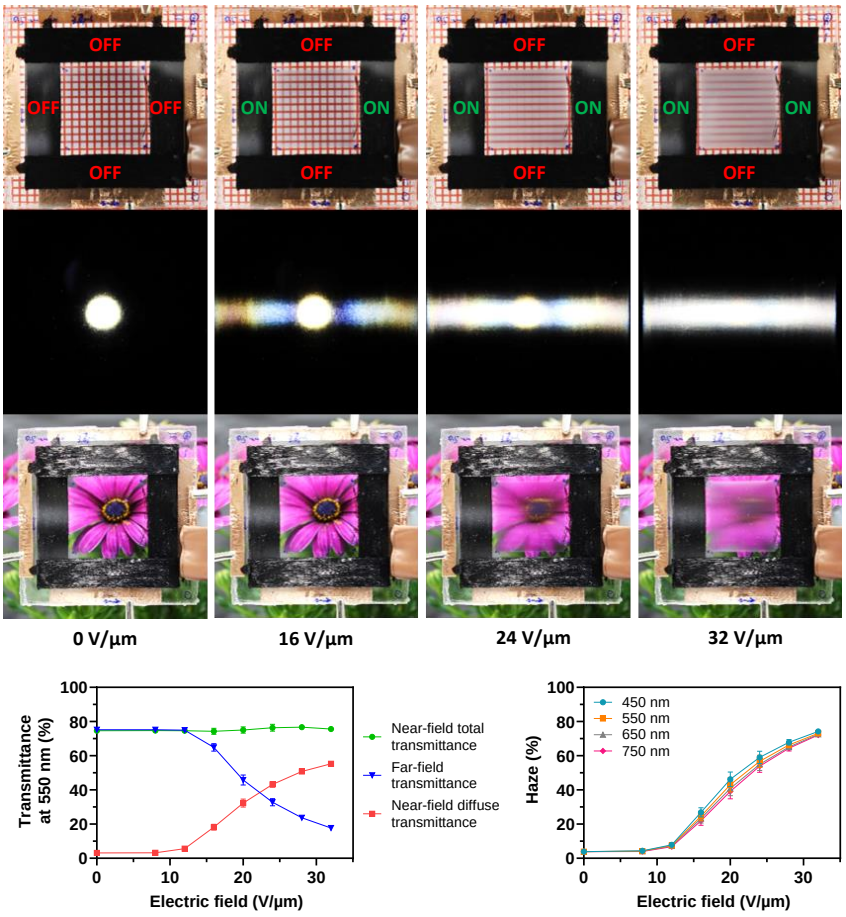

Fig. 7. Electro-optical transduction performance of the bi-directional light scattering device upon activations of the rear layer at increasing electric fields, which progressively compressed the window along the figure's horizontal direction. The images show the device located 3 cm above a grid (whose vertical lines progressively 'vanished'), a light spot (which was re-shaped from a circle to a horizontal line) and a flower (which was blurred horizontally). The graphs present the electrically-induced variations of the transmittances (near-field total, near-field diffuse and far-field) at 550 nm and the dependence on the applied nominal electric field of the Haze number at different wavelengths. Each data point represents the average value from three sample devices. Error bars corresponding to the standard deviation are included, although most of them are too small to be seen.

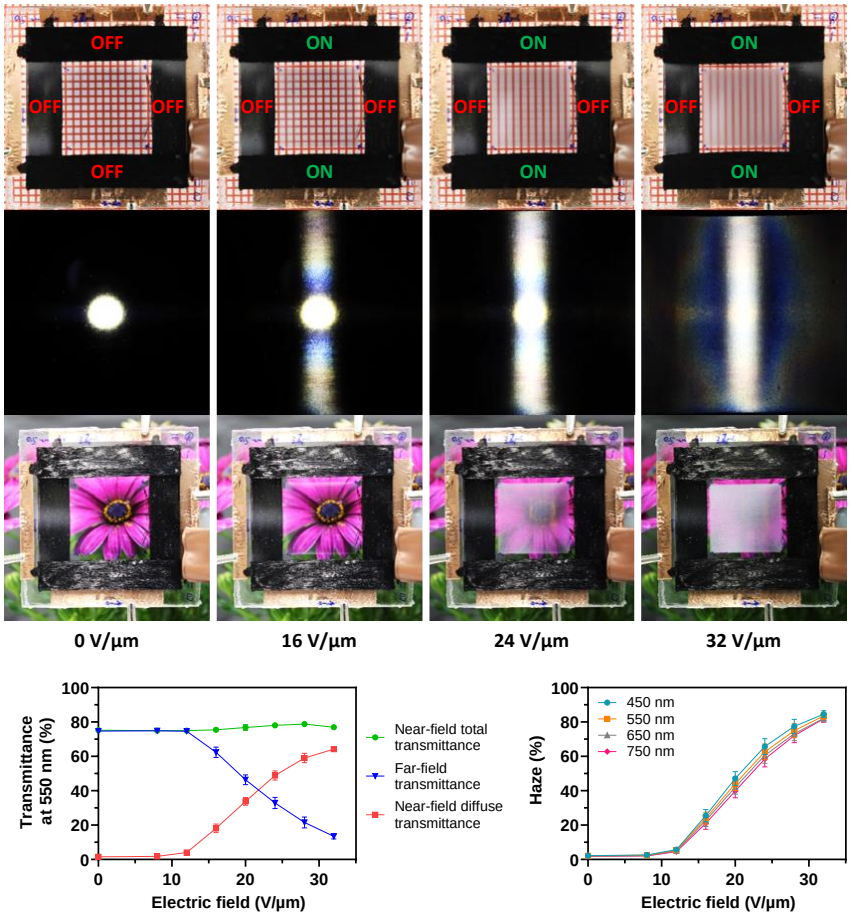

Fig. 8. Electro-optical transduction performance of the bi-directional light scattering device upon activations of the front layer at increasing electric fields, which progressively compressed the window along the figure's vertical direction. The images show the device located 3 cm above a grid (whose horizontal lines progressively 'vanished'), a light spot (which was re-shaped from a circle to a vertical line) and a flower (which was blurred vertically). The graphs present the electrically-induced variations of the transmittances (near-field total, near-field diffuse and far-field) at 550 nm and the dependence on the applied nominal electric field of the Haze number at different wavelengths. Each data point represents the average value from three sample devices. Error bars corresponding to the standard deviation are included, although most of them are too small to be seen.

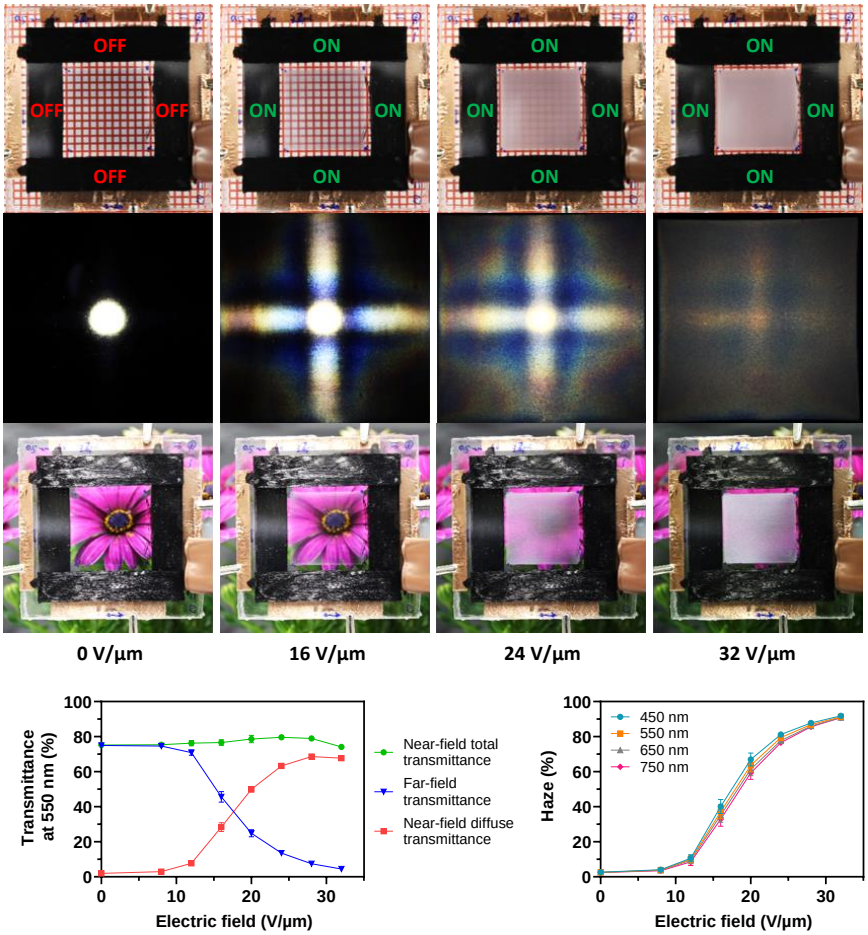

Fig. 9. Electro-optical transduction performance of the bi-directional light scattering device upon activations of the both the rear and front layers at increasing electric fields, which progressively compressed the window along the figure's horizontal and vertical directions. The images show the device located 3 cm above a grid (whose lines progressively 'vanished'), a light spot (which was re-shaped from a circle to a cross) and a flower (which was completely hidden). The graphs present the electrically-induced variations of the transmittances (near-field total, near-field diffuse and far-field) at 550 nm and the dependence on the applied nominal electric field of the Haze number at different wavelengths. Each data point represents the average value from three sample devices. Error bars corresponding to the standard deviation are included, although most of them are too small to be seen.

Whilst the main advantage of this device is a directional control of light scattering, the simultaneous activation of both the layers also offers a broad tuning range of transparency. Indeed, the far-field transmittance at 550 nm could be modulated from 75% down to 4%, corresponding to a variation of the Haze value from 2% to over 90% (Fig. 9).

It is worth noting that overlapping two coated membranes to obtain the bi-directional device forced light to pass through total four layers of PEDOT:PSS coatings. Therefore, as compared to a mono-directional device, the transmittance at electrical rest was inevitably reduced, decreasing from 86% (Fig. 4) to 75% (Figs. 7, 8 and 9). This drawback, however, was not found to particularly impact the quality of the perceived transparency, as demonstrated by the zero-field photos shown in Figs. 7 to 9.

In order to avoid this reduction of transparency resulting from the multi-layer approach, one could envisage a rather different bi-directional device: a single membrane hosting two couples of lateral DEA segments, arranged along two orthogonal directions at the sides of the central window, as represented in Fig. 10.

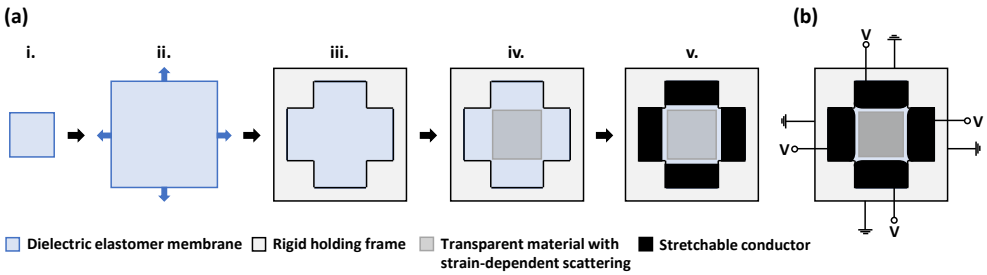

Fig. 10. Possible alternative configuration for a DEA-based bi-directional light scattering device, made of a single elastomer membrane hosting two couples of lateral DEA segments, arranged along two orthogonal directions at the sides of the central window. (a) Fabrication steps from i) a square piece of membrane, which is ii) biaxially pre-stretched (blue arrows), iii) fixed to a rigid holding frame, iv) coated, on both sides, with a transparent material having strain-dependent scattering properties, to create the central tunable window, and v) coated, on both sides, with a non-transparent stretchable conductor, to create lateral DEA segments. (b) Bi-directional operation of the device.

However, that strategy was not adopted in this work, for two main reasons: firstly, it would require a bi-axial pre-stretch, losing the advantage of a uni-axial pre-stretch in terms of maximization of the active strain along the perpendicular direction; secondly, the extension of each DEA segment would be limited to the length of the window's sides, thereby reducing the achievable deformations and making them not uniform along the sides (Fig. 10), degrading the optical effect.

Nevertheless, at least the uniformity of the DEA segments' actuated edges could be restored in such a single-membrane structure, by shaping those edges as curved, rather than straight, so as to make the actuated window exactly square at a given voltage. This would however imply that, to guarantee uniformity, the device could only be used in two states (on and off), rather than with a continuous modulation.

4. Conclusions and future developments

This paper presented the first smart-material-based technology to achieve electrically controllable directional diffusions of light from soft elastomeric membranes. The proposed strategy is based on dielectric elastomer actuation, which is used to achieve anisotropic scattering of light, by electrically tuning the formation of directional wrinkles on the surface of transparent PEDOT:PSS coatings.

The proposed concept was demonstrated with a device made of two overlapped and 90°-shifted layers, capable of both mono- and bi-directional operations: in the former case, an electrical activation of a single layer created wrinkles along one axis, thereby scattering light mostly in the perpendicular direction; in the latter case, both the layers were actuated simultaneously, such that their surfaces became wrinkled along orthogonal axes, inducing bi-directional scattering. This effect could be used, for instance, in automatic directional light beam spreaders for light shaping, in order to electrically spread light in multiple directions dynamically (which might be applied for example to green-screen studios to avoid sharp shadows).

In addition to directional scattering, the prototype device allowed for a significant tuning of transparency, showing an electrical controllability of the far-field transmittance from 75%

down to 4% with a window-to-total area ratio of 1:4. This could be used to electrically vary the transparency of thin soft membranes, with quite a broad tuning range.

The performance of this technology could be further improved by using scattering transparent materials (insulating or not) with higher refractive indexes, in order to increase light scattering when the surface is wrinkled and thus make the transmittance tuning range even broader.

Moreover, the use of membranes made of silicone elastomers is expected to lead to devices with the highest possible response speeds, due to reduced viscoelastic losses [28].

The technology could also be improved to increase the number of degrees of freedom, i.e. the number of selectable directions. This could be achieved by overlapping a larger set of scattering layers with different angular shifts. Nevertheless, any increase of the number of layers should inevitably result from a trade-off between the desirable increase in the range of angles that can be controlled and the disadvantageous reduction of transparency at electrical rest and increase of the overall thickness of the device.

Funding

MSCA-ITN-2014 Marie Sklodowska-Curie Innovative Training Network Programme ("MICACT - MICroACTuators" project, grant agreement 641822).

Acknowledgements

Leihao Chen gratefully acknowledges support from Queen Mary University of London, the China Scholarship Council and the University of Florence.

Disclosure

The authors declare no conflicts of interest.

References

1. M. Williamson and M. Venables, "Special report: 50th Paris air show," Eng. Technol. **8**(7), 18–19 (2013).
2. R. J. Mortimer, D. R. Rosseinsky, and P. M. S. Monk, *Electrochromic Materials and Devices* (John Wiley & Sons, 2015).
3. T. Ohzono, K. Suzuki, T. Yamaguchi, and N. Fukuda, "Tunable optical diffuser based on deformable wrinkles," Adv. Opt. Mater. **1**(5), 374–380 (2013).
4. C. G. Granqvist, "Electrochromic devices," J. Eur. Ceram. Soc. **25**(12), 2907–2912 (2005).
5. G. A. Niklasson and C. G. Granqvist, "Electrochromics for smart windows: thin films of tungsten oxide and nickel oxide, and devices based on these," J. Mater. Chem. **17**(2), 127–156 (2007).
6. C. G. Granqvist, "Electrochromics for smart windows: oxide-based thin films and devices," Thin Solid Films **564**, 1–38 (2014).
7. F. P. Nicoletta, G. Chidichimo, D. Cupelli, G. De Filpo, M. De Benedittis, B. Gabriele, G. Salerno, and A. Fazio, "Electrochromic polymer-dispersed liquid-crystal film: a new bifunctional device," Adv. Funct. Mater. **15**(6), 995–999 (2005).
8. D. Cupelli, F. P. Nicoletta, S. Manfredi, M. Vivacqua, P. Formoso, G. De Filpo, and G. Chidichimo, "Self-adjusting smart windows based on polymer-dispersed liquid crystals," Sol. Energy Mater. Sol. Cells **93**(11), 2008–2012 (2009).
9. M. Kim, K. J. Park, S. Seok, J. M. Ok, H. T. Jung, J. Choe, and D. H. Kim, "Fabrication of microcapsules for dye-doped polymer-dispersed liquid crystal-based smart windows," ACS Appl. Mater. Interfaces **7**(32), 17904–17909 (2015).
10. H. Hosseinzadeh Khaligh, K. Liew, Y. Han, N. M. Abukhdeir, and I. A. Goldthorpe, "Silver nanowire transparent electrodes for liquid crystal-based smart windows," Sol. Energy Mater. Sol. Cells **132**, 337–341 (2015).
11. H.-Y. Ong, M. Shrestha, and G.-K. Lau, "Microscopically crumpled indium-tin-oxide thin films as compliant electrodes with tunable transmittance," Appl. Phys. Lett. **107**(13), 132902 (2015).
12. K.-W. Jun, J.-N. Kim, J.-Y. Jung, and I.-K. Oh, "Wrinkled graphene–AgNWs hybrid electrodes for smart window," Micromachines **8**(2), 43 (2017).
13. M. Shrestha, A. Asundi, and G.-K. Lau, "Smart window based on electric unfolding of microwrinkled TiO2 nanometric films," ACS Photonics **5**(8), 3255–3262 (2018).
14. L. Chen, M. Ghilardi, J. J. C. Busfield, and F. Carpi, "Electrically tuning soft membranes to both a higher and a lower transparency," Sci. Rep. **9**(1), 20125 (2019).
15. D. van den Ende, J.-D. Kamminga, A. Boersma, T. Andritsch, and P. G. Steeneken, "Voltage-controlled surface

wrinkling of elastomeric coatings," Adv. Mater. **25**(25), 3438–3442 (2013).
16. S. Shian and D. R. Clarke, "Electrically tunable window device," Opt. Lett. **41**(6), 1289–1292 (2016).
17. I.-T. Lin, T. Wang, F. Zhang, and S. K. Smoukov, "Fault-tolerant electro-responsive surfaces for dynamic micropattern molds and tunable optics," Sci. Rep. **7**(1), 12481 (2017).
18. S. Shian, P. Kjeer, and D. R. Clarke, "Electric-field induced surface instabilities of soft dielectrics and their effects on optical transmittance and scattering," J. Appl. Phys. **123**(11), 113105 (2018).
19. C. H. Yang, S. Zhou, S. Shian, D. R. Clarke, and Z. Suo, "Organic liquid-crystal devices based on ionic conductors," Mater. Horizons **4**(6), 1102–1109 (2017).
20. F. Carpi, *Electromechanically Active Polymers: A Concise Reference* (Springer International Publishing, 2016).
21. S. Rosset and H. R. Shea, "Flexible and stretchable electrodes for dielectric elastomer actuators," Appl. Phys. A **110**(2), 281–307 (2013).
22. R. Pelrine, R. Kornbluh, Q. Pei, and J. Joseph, "High-speed electrically actuated elastomers with strain greater than 100%," Science **287**(5454), 836–839 (2000).
23. R. E. Pelrine, R. D. Kornbluh, and J. P. Joseph, "Electrostriction of polymer dielectrics with compliant electrodes as a means of actuation," Sensors Actuators A Phys. **64**(1), 77–85 (1998).
24. P. Brochu and Q. Pei, "Advances in dielectric elastomers for actuators and artificial muscles," Macromol. Rapid Commun. **31**(1), 10–36 (2010).
25. F. Carpi, S. Bauer, and D. De Rossi, "Stretching dielectric elastomer performance," Science **330**(6012), 1759–1761 (2010).
26. F. Carpi, D. De Rossi, R. Kornbluh, R. Pelrine, and P. Sommer-Larsen, *Dielectric Elastomers as Electromechanical Transducers: Fundamentals, Materials, Devices, Models and Applications of an Emerging Electroactive Polymer Technology* (Elsevier, 2008).
27. S. J. A. Koh, T. Li, J. Zhou, X. Zhao, W. Hong, J. Zhu, and Z. Suo, "Mechanisms of large actuation strain in dielectric elastomers," J. Polym. Sci. Part B Polym. Phys. **49**(7), 504–515 (2011).
28. L. Maffli, S. Rosset, M. Ghilardi, F. Carpi, and H. Shea, "Ultrafast all-polymer electrically tunable silicone lenses," Adv. Funct. Mater. **25**(11), 1656–1665 (2015).
29. M. Aschwanden and A. Stemmer, "Polymeric, electrically tunable diffraction grating based on artificial muscles," Opt. Lett. **31**(17), 2610 (2006).
30. M. Kollosche, S. Döring, G. Kofod, and J. Stumpe, "A novel approach to tunable diffractive transmission gratings based on dielectric elastomer actuators," Proc. SPIE **7642**, 76422Y (2010).
31. M. B. Krishnan, S. Rosset, S. Bhattacharya, and H. R. Shea, "Fabrication of transmissive dielectric elastomer actuator driven tunable optical gratings with improved tunability," Opt. Eng. **55**(4), 047104 (2016).
32. S. Akbari, S. Rosset, and H. R. Shea, "Improved electromechanical behavior in castable dielectric elastomer actuators," Appl. Phys. Lett. **102**(7), 071906 (2013).
33. D. J. Lipomi, J. A. Lee, M. Vosgueritchian, B. C.-K. Tee, J. A. Bolander, and Z. Bao, "Electronic properties of transparent conductive films of PEDOT:PSS on stretchable substrates," Chem. Mater. **24**(2), 373–382 (2012).
34. J. Liu, N. R. Davis, D. S. Liu, and P. T. Hammond, "Highly transparent mixed electron and proton conducting polymer membranes," J. Mater. Chem. **22**(31), 15534–15539 (2012).
35. M. Vosgueritchian, D. J. Lipomi, and Z. Bao, "Highly conductive and transparent PEDOT:PSS films with a fluorosurfactant for stretchable and flexible transparent electrodes," Adv. Funct. Mater. **22**(2), 421–428 (2012).
36. E. A. Campo, "Physical Properties of Polymeric Materials," in *Selection of Polymeric Materials* (Elsevier, 2008), pp. 175–203.